Journal of CO2 Utilization 92 (2025) 103013

Contents lists available at ScienceDirect

Journal of CO2 Utilization

journal homepage: www.elsevier.com/locate/jcou

Novel comprehensive life cycle assessment (LCA) of sustainable flue gas carbon capture and utilization (CCU) for surfactant and fuel via Fischer-Tropsch synthesis

Jhuma Sadhukhan [a,*], Oliver J. Fisher [b,*], Benjamin Cummings [a], Jin Xuan [a]

[a] Faculty of Engineering and Physical Sciences, University of Surrey, Guildford GU2 7XH, UK
[b] Food Water Waste Research Group, Faculty of Engineering, University of Nottingham, University Park, Nottingham NG7 2RD, UK

ARTICLE INFO

Keywords:
CCUS
CCU
CDU
Carbon dioxide utilization
LCA
Circular carbon economy
Surfactant
High-value product
Product environmental footprint

ABSTRACT

This novel study presents an effective comprehensive life cycle assessment (LCA) of a novel sustainable carbon dioxide capture and utilization (CCU) system to co-produce alcohol ethoxylate (AE7), a valuable surfactant (a high-value chemical component of liquid detergents), and low-medium distillate range liquid fuel. Conventionally, AE7 is produced by reacting fatty alcohols with ethylene oxide from mostly fossil and marginally bio-based resources. This research develops novel AE7 production using carbon sources from flue gas of paper and steel industries, addressing a critical gap in the literature. The core process is Fischer-Tropsch (FT) synthesis using syngas formed by the reverse-water-gas-shift reaction, where recycled CO_2 reacts with H_2. FT produces C11-C13 alkanes and a light-to-medium fuel co-product. The alkanes are converted into C12-C14 fatty alcohols through dehydrogenation, hydroformylation, and hydrogenation. Fatty alcohols react with ethylene oxide to form AE7. The yields (w/w) of AE7 and the fuel co-products are 3.7 % and 3.4 % for paper industry flue gas, and 8.0 % and 9.5 % for steel industry flue gas, respectively. Renewable (wind) electricity meets the hydrogen demand and electricity needs for the reactions, a total of 13.4 and 33.3 kWh/kg flue gas, respectively. The life cycle impact assessment includes global warming potential (GWP) and other impacts using ReCiPe, Impact+ , and Product Environmental Footprint methods. Baseline scenarios show GWP ranging from 2.2 to 3.6 kg CO_2e/kg surfactant for conventional cradle-to-gate AE production systems. The new systems have GWP ranging 0.4–1.3 kg CO_2e/kg flue gas (cradle-to-gate) using mass allocation. Meanwhile, the paper industry's flue gas system has biogenic CO_2, while the steel industry's CO_2 is fossil-based. Considering the GWP reductions due to biogenic CO_2 contents, their overall GWP is 2.56 kg CO_2e and 10.33 kg CO_2e per kg of product (AE7 +fuel) (cradle-to-grave) using economic allocation. Thus, biogenic CCU is critical for the sustainable co-production of high-value surfactants and fuel.

1. Introduction

Surfactants are vital chemical products with a market projected to reach $59.5 billion by 2032 [1]. These amphiphilic molecules reduce surface tension, enabling diverse industrial applications, including detergents, cosmetics, agriculture, and textiles. Nonionic surfactants like alcohol ethoxylates, made from ethoxylated fatty alcohols, are key emulsifiers in products like shampoos and bubble baths [2]. Produced from fossil or bio-based feedstocks, both contribute to environmental impacts, fossil-based surfactants through greenhouse gas (GHG) emissions and bio-based options via deforestation and biodiversity loss. To address environmental challenges, transitioning to a circular carbon economy is essential, where CO_2 is repurposed into chemicals, avoiding additional fossil carbon extraction [3,4]. CO_2 is an abundant, renewable feedstock, but direct air capture remains costly ($100–$600 per ton by 2050) [5]. Capturing CO_2 from industrial emitters with 5 %–40 % CO_2 concentrations, is more cost-effective [3]. Foundational industries like cement, steel, and chemicals, responsible for 10 % of UK emissions, must de-fossilize rapidly to meet the 2050 net-zero target [6]. Industrial CO_2 reuse can mitigate emissions, enhance competitiveness, and secure jobs while driving climate action.

Captured CO_2 from industrial waste gas can be converted into chemical feedstocks through biochemical, chemo-enzymatic, electrochemical, thermocatalytic, photocatalytic or hybrid conversion

* Corresponding authors.
E-mail addresses: j.sadhukhan@surrey.ac.uk (J. Sadhukhan), Oliver.Fisher2@nottingham.ac.uk (O.J. Fisher).

https://doi.org/10.1016/j.jcou.2024.103013
Received 31 October 2024; Received in revised form 18 December 2024; Accepted 27 December 2024
Available online 9 January 2025

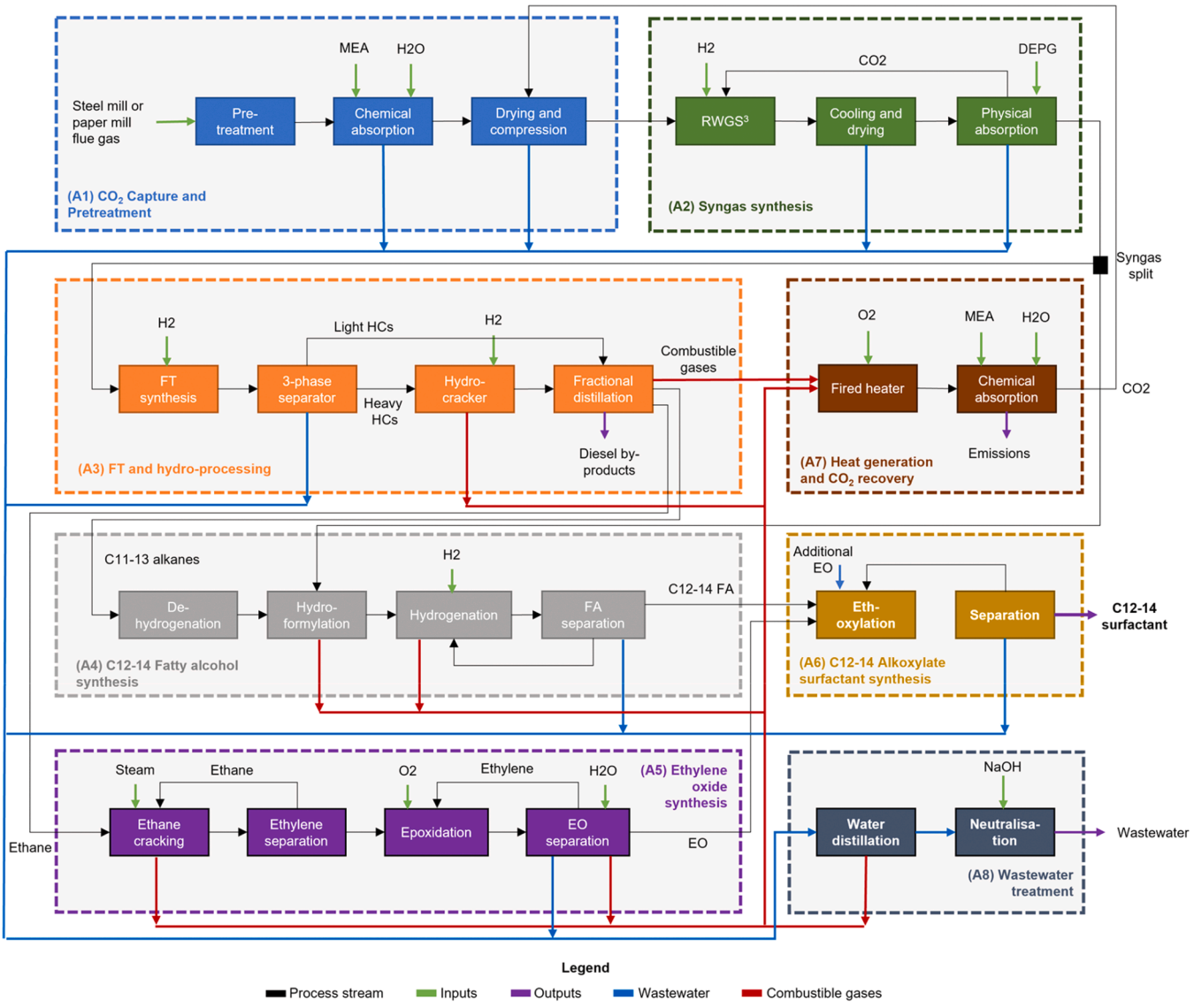

Fig. 1. System block diagram for C12–14 AE7 surfactant production from the steel and paper mill flue gases.

processes [7]. In the biochemical conversion of CO_2, the CO_2 is first captured into a biological system. Then it is converted into value-added products, such as pyruvate or acetyl-CoA, through the use of enzymes or microbial catalysts [8]. Biochemical approaches offer toxicity tolerance but exhibit several disadvantages such as low yield [7]. The chemo-enzymatic is a promising approach that utilizes CO_2 metabolic processes in cells and has several advantages such as higher selectivity and yield, yet unproven for large-scale applications [9]. There remain challenges limiting industrial application, including improving the performance of the various components, such as catalysts and electrodes, and purification of feedstock and product streams [10]. Thermocatalytic approaches for converting CO_2 encompass a broad array of catalytic reactions, such as CO_2 hydrogenation, dry reforming of methane with CO_2, and nonreductive CO_2 conversion into fine chemicals [11]. Among the different CO_2 hydrogenation routes, the reverse water gas shift (RWGS) reaction represents a viable route to convert CO_2 and H_2 into CO and water, and the product CO is then used in downstream Fischer-Tropsch (FT) to produce hydrocarbon products [12]. The RWGS-FT option has been chosen for investigation in this study due to its technological maturity, production capability of a diverse range of products and compatibility with existing infrastructure [13–15]. While studies exist that evaluate the environmental impact of converting CO_2 into gasoline and diesel products via the RWGS-FT route [14,16–20], the life cycle assessment (LCA) of high-value products, like surfactants, production via the RWGS-FT route is not available in the literature. Thus, this is the first LCA study of surfactant production using carbon dioxide capture and utilization (CCU) or carbon dioxide utilization (CDU).

A comprehensive literature review shows only five LCA studies of CO_2 reduction/reuse underpinning the need for LCA methods to benchmark how to conduct LCA of CO_2 reduction/reuse systems. None of these works is dedicated to converting foundational industries' CO_2 emissions into ethoxylated surfactants. Thus, the process investigated is completely novel. In addition, no LCA study explores converting foundational industries' CO_2 emissions into ethoxylated surfactants. Thus, the existing literature only marginally influences this completely novel LCA of CO_2 utilization into surfactants alongside fuel products. Artz et al. (2018) reviewed LCA studies of CO_2-based chemical and fuel syntheses and concluded that replacing energy-intensive routes with carbon dioxide reuse (CDR) is highly promising [21]. The largest positive impact results from the direct incorporation of CO_2 into products. They also concluded the need for LCA methodologies for CDR routes, which this paper fulfils. Sternberg et al. (2017) evaluated the CO_2-based production of formic acid, carbon monoxide, methanol, and methane

using 1 kg of hydrogen, focusing on global warming and fossil depletion impacts [22]. Formic acid production showed the greatest environmental impact reduction, followed by carbon monoxide and methanol, with methane offering the least reduction. Environmental impacts are reduced for hydrogen supplied from renewable electricity-run water electrolysers. Electrochemical conversion of CO_2 into added-value products is gaining popularity and formic acid and acetic acid syntheses by CO_2 utilization using bioelectrochemical technologies have been analyzed for LCA [23,24]. A two-step electrochemical conversion of CO_2 into added-value products has been analyzed for LCA [25]. Their study recognized the importance of intermediates such as syngas from CO_2 for added-value products. Meunier et al. (2020) evaluated CO_2 conversion to methanol through a comprehensive techno-economic and environmental assessment [26]. Their LCA study reveals significant reductions in greenhouse gases compared to conventional fossil-based methanol production. He et al. (2021) explored the environmental benefits of converting CO_2 to syngas via RWGS for liquid fuel and power production [18]. The CO_2 source is a three-stage hydrogen production unit using Fe-based chemical looping combustion, capturing carbon with minimal energy consumption. Carbon emissions primarily stem from natural gas extraction, transportation, and CO_2 recompression. These dedicated LCA studies of CO_2 utilization unequivocally identify the need for more LCA studies of novel CCU or CDU or CDR routes. Chauvy et al. (2020) strongly suggest the need for full LCA to analyze the sustainability of CO_2 utilization systems [27]. In the UK-focused study, Perdan et al. (2017) analyzed the public perception of CO_2 utilization systems from environmental, economic and social perspectives as they approach the commercialization stage [28], which will be important once LCA shows the need for CO_2 utilization in high-value products. In addition to CO_2 utilization, biomass valorization or biorefining is a viable alternative to producing added-value products, such as methanol and dimethyl ether. Liu et al. (2024) presented a sorption-based gasification route to synthesize methanol from biomass via gasification correcting the hydrogen-to-carbon monoxide molar ratio to 2 [29]. Wubulikasimu et al. (2024) showed a CO_2 conversion of 17.4 % and a methanol selectivity of 77.7 % in the CO_2 utilization route [30]. Palomo et al. (2024) proposed a direct dimethyl ether synthesis route to biomass gasification [31], while Vaquerizo and Kiss (2024) evaluated the same route from CO_2 utilization [32]. Biomass being carbon neutral provides climate benefits compared to fossil-based equivalent products. Similarly, biogenic carbon dioxide utilization offers climate impact savings compared to fossil-based carbon dioxide utilization. However, none of these studies conducted a comprehensive LCA to compare biogenic and fossil-based carbon dioxide utilization routes for the same products. Most notably, the literature landscape is yet to see the first-ever novel LCA of surfactant synthesis utilizing biogenic and fossil-based carbon dioxide.

Compared to the RWGS-FT route for synthesizing ethoxylated surfactants [33], methanol or dimethyl ether synthesis routes result in fuel production that accelerates the CO_2 cycle, leading to a faster release of CO_2 back into the atmosphere. Transforming CO_2 emissions from foundational industries into ethoxylated surfactants represents a promising pathway to reducing dependency on fossil-based resources and advancing a circular carbon economy. However, significant environmental challenges must be overcome to enable its commercial deployment. There is currently no LCA of CCU or CDU in high-value surfactant production, presenting a significant research gap in the literature. To address this gap, this study conducts a novel comprehensive LCA for the novel CCU/CDU in surfactant and fuel production for the first time. The primary objective of this study is to evaluate the environmental performance of a novel surfactant supply chain utilizing flue gas-derived CO_2 through a rigorous LCA. Specifically, this study assesses the RWGS-FT route to synthesize ethoxylated surfactants [33] compared to conventional fossil-based and biobased feedstocks. The findings will provide critical insights for industry stakeholders and policymakers regarding the environmental implications of this innovative pathway.

Table 1
Composition of the flue gas from the paper mill plant.

	Recovery boiler	Multi-fuel boiler	Lime kiln	Mix of all 3
NO_x (ppm)	125	150	175	132.1
N_2 (mol%)	67.6	53.4	47.4	64.3
SO_x (ppm)	60	40	50	56.5
H_2O (mol%)	17	32.7	30.9	20.2
CO_2 (mol%)	13	12.1	20.4	13.4
O_2 (mol%)	2.3	1.7	1.2	2.1
Particulates (ppm)	30[a]	15[b]	30[c]	27.8
Flow rate ratio	11.9	2.2	1	

[a] Fly ash mainly Na_2SO_4.
[b] Contains components of Al, Ca and Si.
[c] Fly ash mainly $CaCO_3$.

Table 2
Composition of the flue gas from the steel plant.

	Balance furnace gas	Basic oxygen furnace gas	Coke oven gas	Mix of all 3
N_2 (mol%)	46.6	18.1	5.9	43.3
CO (mol%)	23.5	54	4.1	23.9
CO_2 (mol%)	21.6	20	1.2	20.5
$Ar + O_2$ (mol%)	0.6	0.7	0.2	0.6
H_2 (mol%)	3.7	3.2	60.7	6.5
H_2O (mol%)	4	4	4	4
CH_4 (mol%)	0	0	22	1.1
C_xH_y (mol %)	0	0	3	0.1
Flow rate ratio	20.9	1	1.1	

The paper is structured as follows. First, the process description at a conceptual level is provided. The detailed process optimization study including heat recovery, energy integration, process simulation and techno-economic analysis has already been published [33]. The ISO-standardized LCA methodology implementation is discussed following the process description. Thereafter, baseline and new cases' LCA and uncertainty analyses are discussed, and conclusions are drawn.

2. Methods

2.1. Process description

This research assesses the life cycle impacts of producing C12–14 AE7 surfactants from either paper mills or steel flue gas feedstocks. The process of converting flue gas to surfactant is shown in Fig. 1. The surfactant production consists of eight process areas, namely: CO_2 capture and pretreatment (A1), syngas synthesis (A2), FT and hydroprocessing (A3), C12–14 fatty alcohol synthesis (A4), ethylene oxide synthesis (A5), C12–14 ethoxylated surfactant synthesise (A6), heat generation and CO_2 recovery (A7), and wastewater treatment (A8). Table 5 in Section 3.4 as part of the Results and Discussion in Section 3 shows the net input-output flows of the system in Fig. 1 for life cycle inventory analysis and impact assessment.

The flue gas derived from the paper mill originates mainly from emissions generated by the recovery boiler, multi-fuel boiler, and lime kiln. The paper mill flue gas composition is shown in Table 1 [34]. Three flue gases are produced during conventional steel production: blast furnace gas, basic oxygen furnace gas, and coke oven gas, which are prime feedstocks for the chemical industry due to their relatively high CO, CO_2, or H_2 content [35]. The steel flue gas composition is shown in Table 2.

CO_2 is extracted from the flue gas (A1) through amine scrubbing using monoethanolamine (MEA) chosen for its established industrial

Table 3
A summary of process parameters for the AE7 production system in Fig. 1.

Process Area	Typical Process Conditions				References
	Catalysts	T (°C)	P (bar)	Yield (%)	
A1		20–170	1–25	86	[19,36–40]
A2	$BaCe_{0.2}Zr_{0.6}Y_{0.16}Zn_{0.04}O_3$	600	24.5–30	36	[19,41–43]
A3	Co or Fe	200–360	20–50	52–80	[19,44–48]
A4	Pt, Co, Cr or pincer-ligand-based	500–600	40–300	60–100	[49,50]
A5	Ag	680	20	52–77	[51–53]
A6	KOH-based, or $C_{12}Co_2N_{12}Zn_3$ complex	60–130	15–100		[54,55]
A7		300–500	30–103		[19,47]
A8					[56,57]

efficacy [36]. The MEA solvent absorbs CO_2 from the flue gas yielding a CO_2-rich stream. The CO_2 is compressed in a five-stage compression to 25 bar, given that the primary reactions for FT surfactant production occur under elevated pressure [19]. As the CO_2 undergoes compression, the water vapour is condensed and directed to the wastewater treatment section. Process areas (A1 to A7) are summarized for typical processing conditions in Table 3.

The compressors' isentropic efficiency is 86 %, based on data extracted from relevant literature sources [39,40]. Syngas is produced (A2) via the reverse-water-gas-shift (RWGS) reaction by reacting the captured and recycled CO_2 with H_2 to form CO and H_2O. The RWGS reaction is based on literature results using $BaCe_{0.2}Zr_{0.6}Y_{0.16}Zn_{0.04}O_3$ as the catalyst [41,42]. The RWGS reaction is designed to have a CO_2 conversion ratio of 36 % [43]. The condensed water vapour generated during the RWGS reaction is separated from the syngas through a flasher unit and sent to the wastewater treatment section. The unreacted CO_2 is separated from the syngas via a physical solvent process. In this process, ethylene glycol is employed as the solvent, which absorbs CO_2 [43]. Recycled CO_2 is compressed to 25 bar in a three-stage compression [19].

FT synthesis (A3) is an exothermic process that is used for the catalytic conversion of syngas to higher hydrocarbons and oxygenates [44]. The production of straight-chain paraffins from C1 to C30 is modelled using Eq. (1).

$$nCO + (2n+1)H_2 \quad \rightarrow \quad C_nH_{2n+1} + nH_2O \tag{1}$$

The fractional conversion of each reaction is determined by assessing the weight distribution of each product FT, obtained using the Anderson-Schulz-Flory (ASF) distribution model. A constant chain growth probability, denoted as "α", is assumed in this model. The weight fraction of the FT product, w, is related to the chain growth probability, a, as described in Eq. (2), where *n* denotes the carbon number.

$$w_n = \quad \alpha^{n-1}(1-\alpha)^2 n \tag{2}$$

By applying the ASF relation in Eq. (2), the weight and molar distributions of each FT product are obtained. The hydrocarbons produced from the FT reactor are flashed to separate heavier hydrocarbons (wax) from lighter hydrocarbons. The wax is cooled (to condense the water) to be dried for further hydrocracking, while the lighter hydrocarbons are distilled to produce the C11–13 paraffin for further processing into surfactant, ethane, and liquid fuel by-products. The water produced from the FT synthesis process is separated by flasher and separator after cooling to 50 °C and is subsequently treated by the wastewater treatment process.

The heavier hydrocarbons are hydrocracked; the long-chain, higher-molecular hydrocarbon chains are split into shorter ones through the addition of hydrogen. To maximise these fractions in the product of the hydrocracker, the use of "ideal hydrocracking" is often assumed [45,46]. The yields of the respective cracking products are calculated based on the uniform distribution of the cracking products of the ideal hydrocracking [47,48]. The gas stream is cooled in several stages for energy utilization and the middle distillates are separated off, expanded, and sent to a fractional distillation unit.

C12-C14 fatty alcohol synthesis from C11-C13 alkanes are produced by the dehydrogenation of alkanes into olefins [49], hydroformylation reaction of alkenes into aldehydes [50], and hydrogenation of aldehydes to alcohols [50]. Dehydrogenation of C11-C13 alkanes into C11-C13 alkenes is an energy-intensive process at 500–600 °C using Pt or chromium-based catalyst. An alternative is the high-pressure reaction using pincer-ligand-based catalyst [49]. The final two reactions of hydroformylation and hydrogenation are industrially exploited by BASF, Shell, Exxon, and Sasol in a two-step process using cobalt catalyst [50]. In this system, C11-C13 alkanes are routed from the FT synthesis and hydroprocessing unit to the alkane dehydrogenation process. All the aldehydes formed in the hydroformylation process are hydrogenated into C12-C14 fatty alcohols separated for C12-C14 ethoxylated surfactant production.

Ethylene oxide (EO) is the second reactant required for ethoxylated surfactant synthesis. To produce the required EO the ethane formed from the FT process is first cracked to produce ethylene, which is then reacted with O_2 to form EO. Steam cracking ethane is selected as it is a relatively simple process, involving lower capital costs. Steam and ethane are preheated before entering the cracker [51]. An ethane conversion of 77 % and yield of ethylene of 52 % is typical [52]. The product leaving the steam cracker is used to partly heat the ethane and steam inlet steams to reduce the heating requirements. The steam cracking by-products are separated via distillation and sent to the heat generation and CO_2 recovery process area (A7). The unreacted ethane is recycled to increase overall conversion rates.

The conversion of ethylene to EO is modelled using catalysts such as silver-based catalysts based on reported high selectivity [52,53]. Typical reaction conditions for industrial EO production are assumed using excess ethylene with 8 % conversion of ethylene and 2 % EO in the reactor outlet [53]. The EO is absorbed in water at 20 bar in a counter-current column. The water flow rate is adjusted to achieve total recovery of the diluted EO. The EO is then desorbed under lower pressure, reaching a purity of 99 % [53]. The wastewater is sent to the wastewater treatment section. The gas stream leaving the absorber, which is depleted in EO, is split into three streams: a fraction of the stream is sent to the CO_2 removal section, whereas the rest is directly recycled to the reactor to limit separation costs and increase overall conversion rates [53]. A small fraction (<1 %) of the gas stream from A5 is purged to avoid the build-up of impurities.

Alkoxylation is the reaction of EO with a long-chain alcohol, catalyzed by homogenous catalysts to produce the ethoxylated surfactant. Typically, alkoxylation reactions are generally performed in semi-batch gas-liquid reactors [54]. However, recent research and patents have focused on developing continuous reactors for alkoxylation due to improved safety and efficiency considerations [54]. A continuous stirred tank reactor has been modelled [55] owing to the lower temperature requirements of other continuous methods [54].

All combustible waste gases from the reaction areas are combusted to recover and supply heat for the process [47]. Wastewaters containing organic solvents, such as alcohol and halogenated solvents, must be treated to remove the volatile polluting compounds before being sent to

the wastewater treatment for regulated water discharge into the water sources. Volatile organic compounds (VOCs) are compounds that have a high vapour pressure and low water solubility that have significant adverse effects on human health [56]. These VOCs from wastewater can enter the atmosphere through air-water exchange and must be removed before further treatment. Contaminated VOCs are recovered and reused for heat generation [57]. The water is sent as a reflux system to the top of a distillation column to maximise VOC recovery. The VOCs are incinerated, and heat is recovered before being released into the air. The bottom product is then sent for further wastewater treatment.

The entire process has been simulated using integrated modeling tools to analyze the interconnectivity of process steps. These models incorporate energy, mass, and cost flows, and their in-process integration and optimization, allowing for a holistic process optimization [33]. Our previous publication [33] dedicates a section to the energy integration of the Fischer-Tropsch (FT) process, focusing on optimizing heat recovery and reuse. Advanced heat integration models have been employed to evaluate the coupling of heat from exothermic FT reactions to upstream and downstream processes. For instance, low-grade heat is redirected to assist in CO_2 capture by monoethanolamine (MEA) absorption process, while high-grade heat is utilized for steam generation, ensuring no heat loss. To substantiate these findings, pinch analysis techniques were employed to map the thermal energy flows and identify areas for improvement in the carbon capture and storage (CCS) system using MEA-based absorption. Sadhukhan et al. (2014) simulated with energy integration the MEA-based absorption process for CCS [38]. The absorption and solvent regeneration columns work at high-pressure-low-temperature and low-pressure-high-temperature operating conditions. Their opposite operating principles allow heat and work integration between them, i.e., pre-cooling and pressurizing pure MEA (recovered + recycled MEA with make-up MEA) before entering the absorption column through heat and work exchange with spent MEA before entering the regeneration column. This not only maximizes the energy efficiency and minimizes the make-up MEA, but the absorption-based CCS system also becomes the net heat source. Our preceding publications [33,38] have rigorously addressed these concerns through detailed optimization analyses, advanced simulation modeling using Aspen Plus, strategic process integration and techno-economic optimization. The optimal foreground system's input-output inventory flows resulting from our whole process system optimization studies [33,38] provide a solid foundation for this LCA study towards industrial implementation. Thus, this study focuses on LCA building on the whole process system optimization studies [33,38].

2.2. Life cycle assessment

LCA (ISO14040–44) has been accepted as a standard tool [38] to predict the life cycle global warming potential (GWP) [58] and other environmental impacts [59] of systems, to compare the environmental sustainability between new and existing systems. A range of impact categories using the various standard life cycle impact assessment (LCIA) methods, ReCiPe Midpoint (M) Hierarchist (H) [60], Impact+ [61] and Product Environmental Footprint [62] including the IPCC global warming potential (GWP) [63]. ReCiPe (M) (H) is the globally accepted LCIA method with the global consensus on their characterisation factors of pollutants and resources and impact categories [38,60]. Impact+ [61] and Product Environmental Footprint [62] are particularly relevant for Europe [38]. The European Commission is keen to mainstream the Product Environmental Footprint for LCIA [62]. The new system's LCA must consider the future renewable energy provision for feasibility, similar to [64,65]. The new systems' GWP must be compared against a baseline to benchmark.

The baseline scenario has been drawn from all plausible existing surfactant-producing systems. The whole range of existing surfactant production systems available in Ecoinvent 3.10 and Industry Data 2.0 comprise the baseline systems. As they are only needed as the baseline to compare the new system's performance, their detailed assumptions are not shown. Their database names are provided because the information including assumption conditions is proprietary to the providers. Providing the life cycle inventory database names is an acceptable norm in the LCA literature. As all plausible existing surfactant production databases have been evaluated for LCIA, their entire distribution or range has been captured, leaving behind no scenario from this benchmarking analysis. SimaPro 9.6 [66,67] is applied to generate all the LCA study results.

Table 4
Ecoinvent 3.10 AE production databases.

Context	Type of AE	Feedstock
RER or ROW	AE3	petrochemical, coconut oil, and palm kernel oil
Cut-off or APOS	AE7	petrochemical, coconut oil, and palm kernel oil
or Conseq	AE11	palm oil

LCA comprises four interactive stages, goal and scope definition, inventory analysis, impact assessment and interpretation. The goal and scope definition includes the functional unit, system boundary and system definitions. The functional unit is a 1 kg ethoxylated surfactant (AE) production from all the baseline systems considered. The functional unit for the new system's LCIA reporting could take various bases. For example, one of the drivers for the new system is CCU/CDU or flue gas utilization; thus, one unit of flue gas can be chosen to report the LCIA results, i.e., 1 kg flue gas. A mass allocation approach is applied for LCIA of 1 kg flue gas reuse, e.g., in kg CO_2e/kg flue gas for GWP. The functional unit for the new system can also be 1 kg AE7 surfactant production to compare against baseline systems e.g., in kg CO_2e/kg AE7 for GWP, in which case, an economic allocation approach is applied. In the economic allocation, the total impacts in each category can be allocated to AE7 or the marketable products including AE7 and the co-product fuel. The other coproduct of flue gas utilization is a liquid fuel in the low-to-medium distillate range. Thus, the total impacts in each category can be allocated to AE7 and the co-product fuel, which is another economic allocation approach. The LCIA of the baseline and new systems is shown for the cradle-to-gate systems. Later on, the gate-to-grave system is considered for the cradle-to-grave GWP of our novel system. For the gate-to-grave system, only the nature of the embedded carbon in the products, i.e., fossil-based (in the case of steel industries' flue gas utilization) or biogenic (in the case of paper industries' flue gas utilization), has been considered, either to add the fossil-based carbon dioxide or subtract the biogenic carbon dioxide to the cradle-to-gate GWP of our novel system.

The foreground new system, discussed in Section 2.1, has been considered up to the plant gate, i.e., AE7 product. The foreground system's external energy and material flow requirements are assigned with cradle-to-grave background life cycle inventory data. The same system boundary principles are applied to the baseline systems. The scope of the systems under consideration is global meaning that the global supply chains are considered. In addition, consequential scenarios are drawn to show improvements in the environmental profiles of the new systems. Hot spots are analyzed for the various systems under consideration. As mentioned above, GWP is the main life cycle impact considered, while ReCiPe, Impact+ and Product Environmental Footprints are applied as appropriate to show any potential tradeoffs.

Life cycle inventory data are extracted from Ecoinvent 3.10. Additionally, Industry Data 2.0 is considered to evaluate two more systems as the baseline. There are 42 Ecoinvent 3.10 baseline databases identified for conventional AE production as the benchmark. The datasets range Europe (RER) and the rest of the world (ROW) systems in the cut-off (recycle streams carry no impact forward), at-the-point-of-substitution (APOS) (recycle streams carry impacts forward, and consequential (Conseq) (future supply chains) scenarios producing three types of AE (AE3, AE7 and AE11, where, in AE7, as shown in Table 4. Palm oil only gives AE11 among the given petrochemical, coconut oil, palm oil and

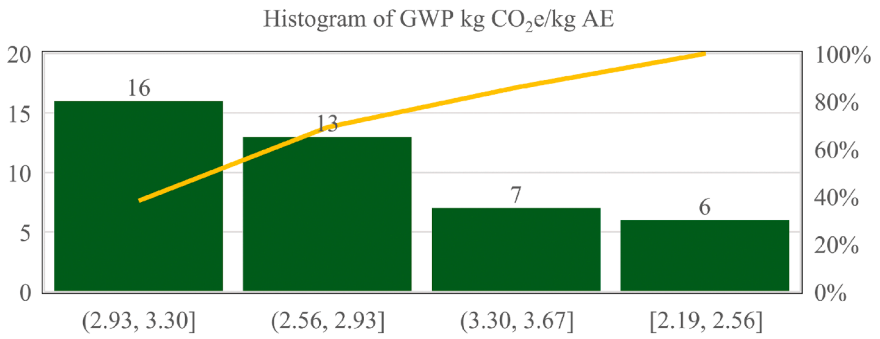

Fig. 2. GWP histogram of all 42 Ecoinvent 3.10 AE-producing databases.

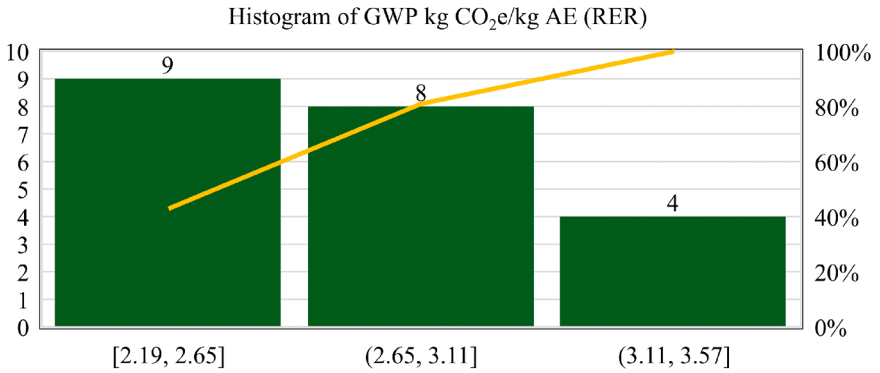

Fig. 3. GWP histogram of 21 Ecoinvent 3.10 AE-producing (RER) databases.

palm kernel oil feedstocks under consideration for the baseline scenarios. Thus, for AE3 and AE7, there are 18 databases each, totalling 36 databases. For AE11, there are 6 databases. They total to 42 databases.

As the study is based in the European region, RER-based systems are further analysed for GWP (21 databases). This means that the plant location is in the RER/EU region, while its supply chain scopes are global depending on where its raw material supplies are sourced from in the existing databases. The GWP results are analyzed for potential ranking between systems and hotspots within the systems (cradle-to-gate). Furthermore, 6 AE7-producing and 1 AE11-producing baseline systems in RER are zoomed into for the full LCIA profiles. These are:

1) fatty alcohol and ethylene oxide from petrochemicals (AE7, Cut-off)
2) fatty alcohol from coconut oil and ethylene oxide from petrochemicals (AE7, APOS)
3) fatty alcohol from palm kernel oil and ethylene oxide from petrochemicals (AE7, Cut-off)
4) fatty alcohol from palm oil and ethylene oxide from petrochemicals (AE11, Cut-off)

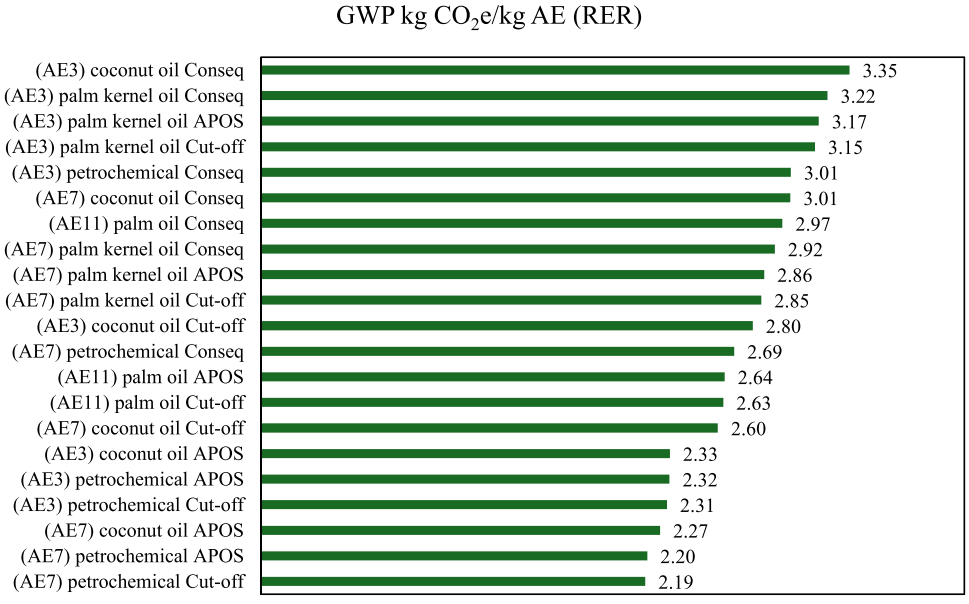

Fig. 4. GWP of 21 Ecoinvent 3.10 AE-producing (RER) databases.

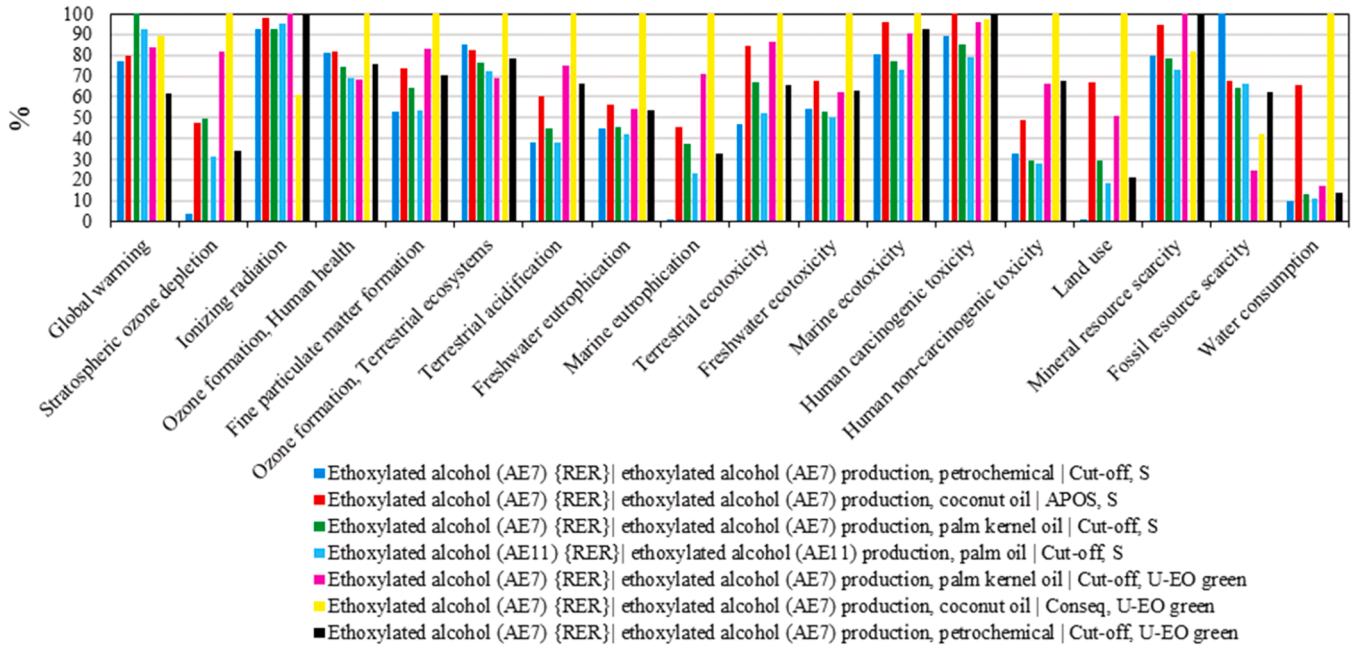

Fig. 5. Environmental profile comparisons between seven baseline systems for AE7 production in RER (ReCiPe (M) (H)).

5) fatty alcohol from palm kernel oil and green (bio-based) ethylene oxide (AE7, Cut-off)
6) fatty alcohol from coconut oil and green (bio-based) ethylene oxide (AE7, Conseq)
7) fatty alcohol from petrochemicals and green (bio-based) ethylene oxide (AE7, Cut-off)

The new green (bio-based) ethylene oxide inventory data is given in the Supplementary Information. The two databases from Industry Data 2.0, C12–14 Alcohol (oleo) Ethoxylate and C12–15 Alcohol (petro) Ethoxylate, are also added to the baseline cases. The Supplementary Information shows their assumption bases, such as hotspots and their geographic locations. The Industry Data 2.0 databases are:

8) "Alcohol (oleo) Ethoxylate, 7 moles EO (No. 10 - Matrix), at plant, 100 % active ingredient /EU-27"
9) "C12–15 Alcohol (petro) Ethoxylate, 7 moles EO (No. 12 - Matrix), at plant, 100 % active ingredient/EU-27"

3. Results and discussion

3.1. LCIA of baseline cradle-to-gate systems

This subsection shows the LCIA of the baseline cradle-to-gate systems considered in this study. GWP is predicted for the 42 Ecoinvent 3.10 AE-producing databases. Fig. 2 shows the GWP histogram of 42 cases. There are 7 systems with GWP values greater than 3.3 kg CO_2e/kg AE, 16 systems with 2.93–3.3 kg CO_2e/kg AE, 13 systems with 2.56–2.93 kg

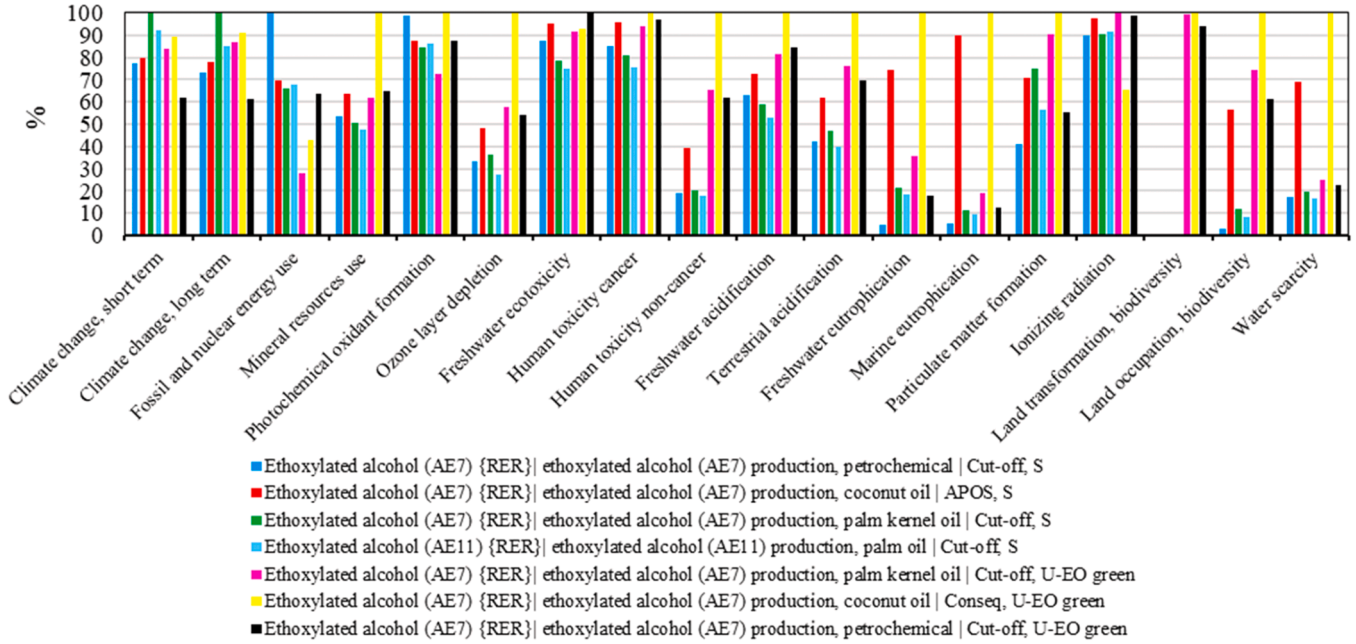

Fig. 6. Environmental profile comparisons between seven baseline systems for AE7 production in RER (Impact+).

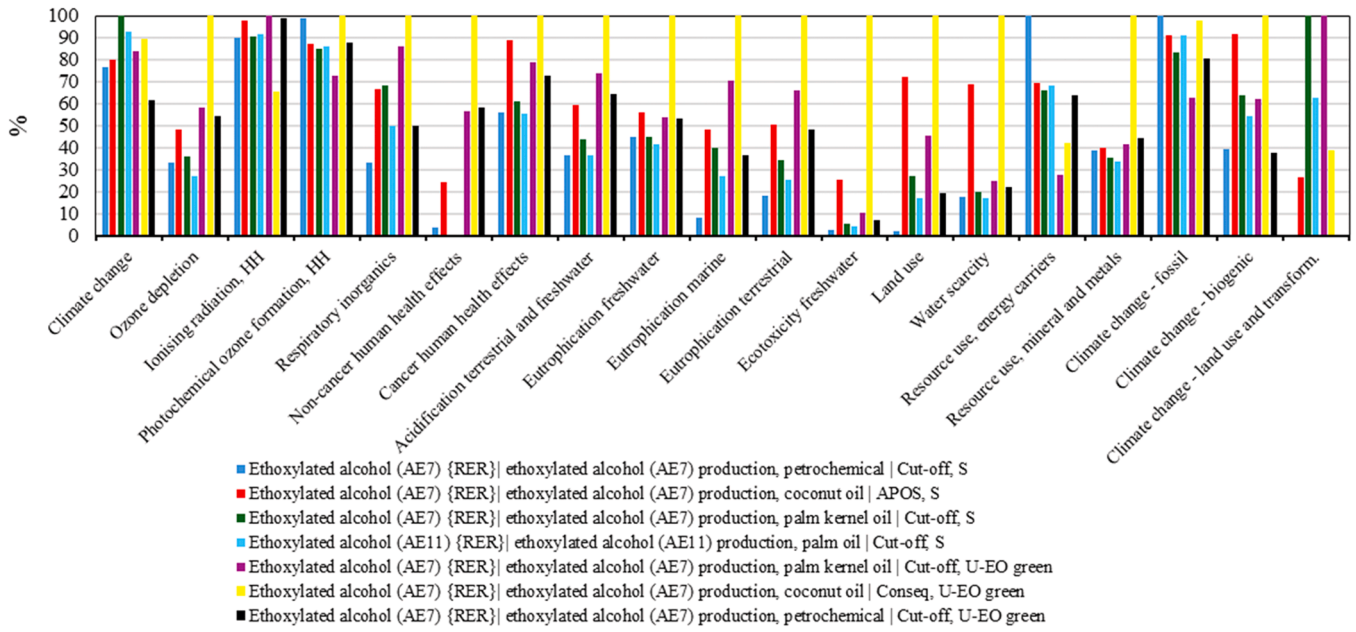

Fig. 7. Environmental profile comparisons between seven baseline systems for AE7 production in RER (Environmental Footprint).

CO_2e/kg AE, and 6 systems with 2.19–2.56 kg CO_2e/kg AE.

Fig. 3 shows the GWP histogram of 21 RER cases. There are 4 systems with GWP values greater than 3.11 kg CO_2e/kg AE, 8 systems with 2.65–3.11 kg CO_2e/kg AE, and 9 systems with 2.19–2.65 kg CO_2e/kg AE.

The following observations are made.

1) AE7-producing systems have the least GWP.
2) The increasing order of GWP impacts per kg of AE is: AE7 < AE3 < AE11.
3) AE11 is only produced from palm oil.
4) The increasing order of GWP impacts in the context of the systems is: Cut-off < APOS < Conseq.
5) The increasing order of GWP impacts for various feedstocks is: petrochemical < coconut oil < palm kernel oil < palm oil (Fig. 4).

The hotspot analyses, illustrated in the Supplementary Information, show the following observations.

1) Similar GWP contributions between the two reactants (fatty alcohol and ethylene oxide) for the petrochemical-based systems (Figure A1)
2) Similar GWP contributions between the two reactants, fatty alcohol from coconut oil and ethylene oxide from petrochemicals (Figure A2)
   a. Within the coconut oil production, land use changes due to clear-cutting primary and secondary forests have the highest GWP contribution (Figure A3)
3) Fatty alcohol from palm kernel oil has a higher GWP than ethylene oxide from petrochemicals making up AE7 (Figure A4)
   a. Within the palm kernel oil production, palm fruit bunch production impacting land use change has the highest GWP contribution (Figure A5)
4) Similar GWP contributions between the two reactants (fatty alcohol and ethylene oxide) for AE11 production (Figure A6)
   a. Within the palm oil production, palm fruit bunch production impacting land use changes has the highest GWP contribution (Figure A7)

Fig. 5 shows the ReCiPe (M) (H) methodology-derived environmental profiles (in 0–100 scales) of the seven baseline systems in RER. Fig. 6 shows the Impact+ methodology-derived environmental profiles (in 0–100 scales) of the seven baseline systems in RER. Fig. 7 shows the Environmental Footprint methodology-derived environmental profiles (in 0–100 scales) of the seven baseline systems in RER. The results in terms of trends of these three LCIA methodologies are aligned, despite the differences in units of their impact categories. The results thus show the robustness. GWP is the lowest for fatty alcohol from petrochemicals and green (bio-based) ethylene oxide – this case is also better performing in land use and water consumption compared to most systems. In the fossil resource depletion and ozone formation categories, the AE7 production system from fatty alcohol from palm kernel oil and green (bio-based) ethylene oxide has the least impact. The AE7 production systems from fatty alcohol from coconut oil and green (bio-based) or petrochemical-based ethylene oxide are not attractive in any environmental categories. The AE11 production system from fatty alcohol from palm oil and petrochemical-based ethylene oxide has the least impact in the human toxicity, marine ecotoxicity and freshwater eutrophication categories.

The GWP of the cradle-to-grave petrochemical-based AE7 system is however inevitably greater than that of the bio-based AE7 system because of the release of fossil-based carbon dioxide to the atmosphere at the end-of-life of AE7 in the former system and the release of biogenic carbon dioxide to the atmosphere at the end-of-life of AE7 in the latter system. The biogenic carbon dioxide released into the atmosphere has a faster sequestration cycle during biomass growth, neutralising the atmospheric carbon dioxide. Thus, the fossil-based carbon dioxide released into the atmosphere at the end-of-life of AE7 is added to the cradle-to-gate GWP of the petrochemical-based AE7 system, while the biogenic carbon dioxide released into the atmosphere at the end-of-life of AE7 is subtracted to the cradle-to-gate GWP of the bio-based AE7 system, ultimately resulting in a lower GWP for the cradle-to-grave bio-based AE7 system compared to the cradle-to-grave fossil-based AE7 system. Thus, despite greater land use potential impacts, the cradle-to-grave bio-based AE7 system is an overall winner (best) baseline system. Neither the Ecoinvent nor the Industry 2.0 indicates the gate-to-grave life cycle inventories of AE7 systems. To complement this data gap, this study accounts for the embedded carbon content in AE7 (fossil-based or biogenic) to calculate the gate-to-grave embodied GWP of our new AE7 system, shown in the final discussion of the next section.

Furthermore, Table A2 shows the ReCiPe (M) (H) LCIA results of two AE7-producing baseline systems from Industry Data 2.0 in the

Table 5
The net input-output flow inventory data of the AE7 production system (Fig. 1) from 1 kg industrial flue gas.

	Paper Industry	Steel Industry	Unit
Input			
Ethylene oxide	0.01	0.066	kg
Carbon dioxide	0.2086	0.3102	kg
Oxygen	0.1499	0.6063	kg
Monoethanolamine solvent	0.0032	0.0119	kg
Electricity	13.37	33.33	kWh
Emissions			
To Air			
Carbon dioxide	0.0076	0.1134	kg
Nitrogen dioxide	7.90E−06		kg
Sulphur dioxide	8.50E−06		kg
To Water			
Chemically polluted water	0.1443	0.7121	kg
Carbon dioxide	0.00226	0.00385	kg
To soil			
Silicon	2.50E−07		kg
Aluminium	2.50E−07		kg
Calcium	2.50E−07		kg

Supplementary Information. The two datasets selected are C12–14 "Alcohol (oleo) Ethoxylate, 7 moles EO (No. 10 - Matrix), at plant, 100 % active ingredient /EU-27" and "C12–15 Alcohol (petro) Ethoxylate, 7 moles EO (No. 12 - Matrix), at plant, 100 % active ingredient/EU-27". Their GWP is 3.36 and 2.38 kg CO_2e/kg AE, which are within the range of the Ecoinvent 3.10 databases' GWP predictions (Fig. 4). Their normalized comparison is shown in Figure A8 in the Supplementary Information. Except for some categories, the fossil-based AE7 production system is better than the oleo-based AE7 production system (cradle-to-gate). It must be noted that the cradle-to-grave fossil-based AE7 production system is not better than the cradle-to-grave (bio) oleo-based AE7 production system. Because the former releases fossil-based carbon dioxide upon post-life biodegradability, which is a regulatory requirement for surfactants (AE7). The latter releases biogenic carbon dioxide upon post-life biodegradability and the biogenic carbon dioxide from the atmosphere is sequestered during biomass growth, thus closing the cycle. Overall, considering all the database systems for AE production as a baseline/benchmark ensures the comprehensiveness of comparing the new system's LCIA.

3.2. *LCIA of AE production from this study's novel flue gas systems*

This section discusses the LCIA of the new AE production system, i.e., AE7 production from industrial flue gas systems sourced from the paper and steel industries. The net input-output foreground flow inventory data of the AE7 production systems from industrial flue gas extracted from our previous process simulation, optimization and techno-economic analysis study [33] are shown in Table 5.

For each net input inventory flow needed including the flue gas, the cradle-to-grave life cycle inventory data is extracted from Ecoinvent 3.10 Cut-off to conduct the LCIA. The overall system is thus cradle-to-gate up to the production of AE7. The functional units selected to report the LCIA results are 1 kg of flue gas utilization as its use to added-value production for a circular economy is a driver for this study (mass allocation), and 1 kg of marketable products bearing all the burden and

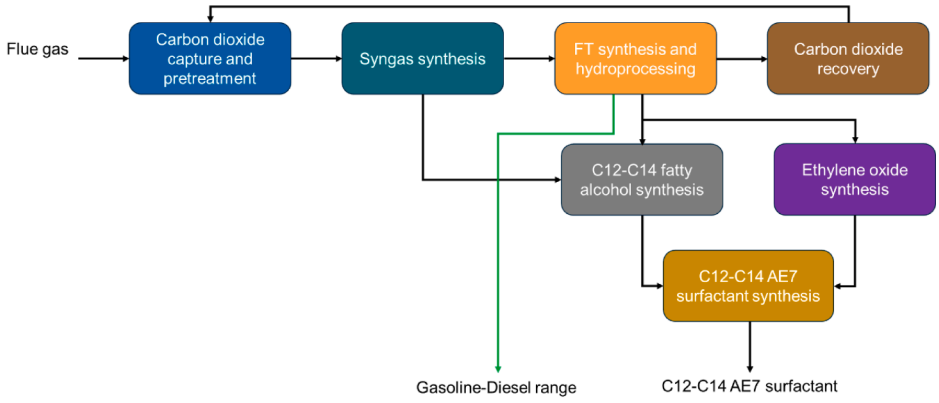

	Paper industry	**Steel industry**
Flue gas mass input, tonne	1	1
CO_2 mass fraction in flue gas	0.21	0.31
CO mass fraction in flue gas	0	0.23
Carbon in flue gas (mass fraction)	0.06	0.18
C12-C14 ethoxylated (AE7) surfactant yield, % of flue gas	3.7	8
Mass fraction of AE7 C12EO7 C13EO7 C14EO7	0.34 0.34 0.32	0.35 0.35 0.3
Fuel yield, % of flue gas	3.4	9.5
Net energy requirements, MWh	13.37	33.33
Carbon utilisation in ethoxylated (AE7) surfactant (fraction)	0.47	0.32
Carbon utilisation in gasoline-diesel range yield (fraction)	0.5	0.43

Fig. 8. Overall block diagram (top) and a summary of the main flows (bottom).

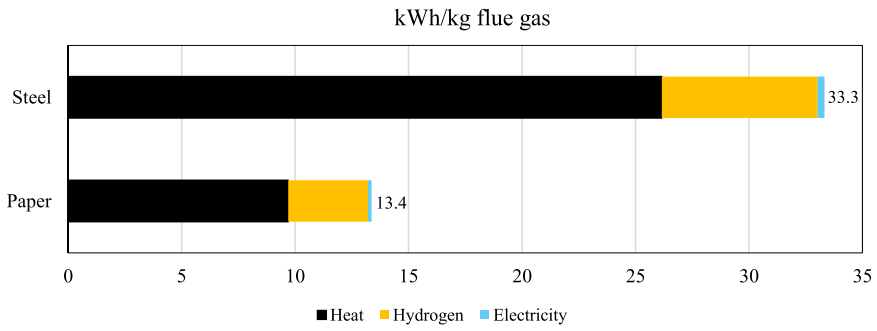

Fig. 9. Electrical energy distributions to meet the heat, hydrogen, and electricity requirements.

1 kg of AE7 production as it is a target product bearing all the burden (economic allocation). Moreover, the least environmental impact incurring energy systems are selected, i.e., wind electricity [68,69], heat from electrolytic hydrogen run with wind electricity [70,71], and wind electricity to supply electrolytic hydrogen as a reactant or raw material for the reactions. Wind electricity is the least impact renewable energy to provide not only electricity but also heat and hydrogen, through electrolytic hydrogen production [60]. Net emissions (Output – Input) or net raw material inputs after in-process recycling are considered for each material. Net amine input or make-up is considered. Monoethanolamine is the solvent to recover carbon dioxide from the flue gas [38]. Thus, energy-integrated absorption and solvent regeneration/recovery units are considered [38]. Similarly, make-up ethylene oxide after in-process recycling is considered. The net input and output inventory flow data mapping against Ecoinvent 3.10 Cut-off databases for 1 kg AE7 surfactant production from the industrial flue gas is shown in the Supplementary Information (Figs. A9–10 for paper and steel industry flue gases, respectively) (the basis is 1 kg industrial flue gas). For the embedded environmental footprint of the flue gas input to the systems, the global average market data of Ecoinvent has been considered. All the input databases selected are cut-off databases. Fig. 8 shows the overall block diagram (a simplified version of Fig. 1) and overall marketable product (AE7 surfactant and liquid fuel range) yields. To simplify, the block diagram does not show the heat and water recovery units' interactions with other units (as in Fig. 1), detailed in our earlier publication [33]. The table below the block diagram shows the flue gas, product, and net energy specifications.

It can be noted that the carbon utilization factor (ratio between carbon in the products and carbon in carbon dioxide and carbon monoxide in the flue gas) is higher in the case of the paper industry (0.97) than in the case of the steel industry (0.75), despite the greater carbon input via carbon monoxide in the latter. The energy requirement is also lower in the former. The energy requirement increases considerably with higher carbon input to make the products. To calculate the energy requirements, the plants are assumed to run on the least impact renewable energy system, i.e., wind electricity [60]. Fuel gas generated has been utilized in-process to supply combined heat and power and internal process-to-process heat recovery has also been considered [72,73]. External energy, utility, and raw material requirements are minimized [38,74]. The unmet heat, hydrogen and electricity requirements are met by external wind electricity. The net electricity needed to run the paper and steel industries' flue gas utilization systems is 13.37 and 33.33 kWh/kg flue gas. Fig. 9 shows the distribution of electrical energy to meet the heat, hydrogen, and electricity required by the two systems. Heat and hydrogen requirements are the electrical energy-consuming hotspots 72–78 % and 20–26 %, respectively. Overall, the paper industry flue gas utilization system is seen to be more efficient. In addition, carbon in the paper industry flue gas is biogenic contrary to fossil-based carbon in the steel industry flue gas.

The location of the plant is assumed to be in the UK (wind electricity supply), while the net input flows' supply chains are global [60]. The impact assessment was performed using ReCiPe (M) (H). As for the baseline systems, the ReCiPe (M) (H), Impact+ and Product Environmental Footprint methodologies generated aligned LCIA profiles, in this

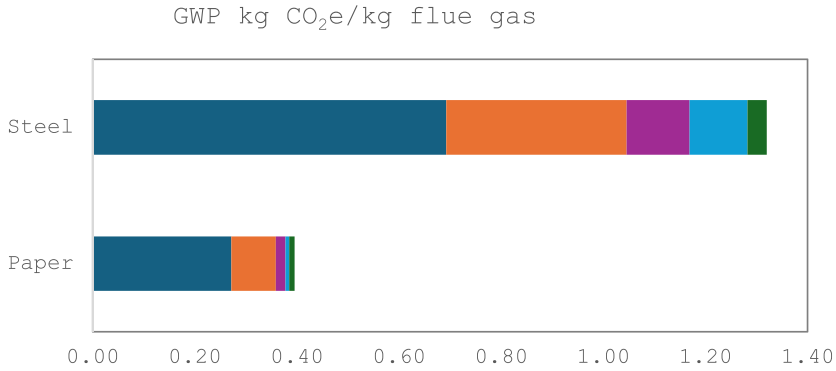

	Paper	Steel
Electricity	0.27	0.69
Oxygen	0.09	0.35
Ethylene oxide	0.02	0.12
Emissions	0.01	0.11
MEA	0.01	0.04

Fig. 10. GWP comparison between the paper and steel industries' 1 kg flue gas utilization cradle-to-gate systems. The figure shows the detailed breakup of GWP contributions (kg CO_2e/kg flue gas) of the input materials and energy and output emissions. The GHG emission can be seen in Table 5.

Table 6
GWP comparisons between the paper and steel industries' flue gas utilization systems. The allocations that show lower GWP than the baseline scenarios are highlighted in green.

GWP kg CO_2e	Basis	Paper	Steel
Mass allocation	per kg flue gas	0.40	1.32
Economic allocation to product	per kg product	5.57	7.51
Economic allocation to AE7	per kg AE7	11.61	16.34
Mass allocation to CO_2 and CO in flue gas	per kg CO_2 + CO in the flue gas	1.89	2.44
Mass allocation to CO_2 and CO utilization	per kg CO_2 + CO utilization	1.95	3.25

case, the globally accepted ReCiPe (M) (H) has been applied. The results of the full LCIA ReCiPe (M) (H) profiles for the paper and steel industries' flue gas utilization systems are shown in the Supplementary Information (Table A3). Fig. 10 shows the GWP comparison between the paper and steel industries' 1 kg flue gas utilization systems. The steel industries' flue gas utilization system incurs greater GWP than the paper industries' flue gas utilization system. The hotspots are electricity > oxygen > ethylene oxide > emissions > monoethanolamine. The CO_2 global market Ecoinvent cut-off data carries no burden from the upstream.

3.3. Interpretation: allocation and uncertainty analysis

The results of the mass and economic allocation approaches are summarized in Table 6. The quantities of marketable useful products, AE7 and low-to-medium range fuel, from the paper and steel industries' flue gas utilization systems, are 0.07 and 0.18 kg/kg flue gas (Fig. 8). With mass-based allocation, the total GWP impacts of the paper and steel industries' flue gas utilization systems are viable (0.4 and 1.32 kg CO_2e/kg flue gas). With the economic allocation of the total GWP to the marketable products (assumed to have similar market price), the GWP is

Table 7
Monte Carlo simulation results of full ReCiPe (M) (H) LCIA profile of cradle-to-gate flue gas utilization systems. Basis: 1 kg flue gas (top: steel industry; bottom: paper industry).

Impact category	Unit	Mean	Median	SD	CV	2.50 %	97.50 %	SEM
Steel industry								
Fine particulate matter formation	kg PM2.5 eq	2.21E−03	2.20E−03	1.07E−03	4.86E+ 01	9.38E−05	4.33E−03	1.07E−05
Fossil resource scarcity	kg oil eq	3.63E−01	3.59E−01	7.79E−01	2.14E+ 02	−1.17E+ 00	1.91E+ 00	7.79E−03
Freshwater ecotoxicity	kg 1,4-DCB	1.60E+ 00	1.60E+ 00	4.50E−02	2.81E+ 00	1.51E+ 00	1.69E+ 00	4.50E−04
Freshwater eutrophication	kg P eq	1.10E−03	1.10E−03	4.45E−04	4.06E+ 01	2.17E−04	1.97E−03	4.45E−06
Global warming	kg CO_2 eq	1.33E+ 00	1.32E+ 00	1.20E+ 00	9.05E+ 01	−1.02E+ 00	3.70E+ 00	1.20E−02
Human carcinogenic toxicity	kg 1,4-DCB	6.37E−01	6.37E−01	5.42E−02	8.51E+ 00	5.30E−01	7.45E−01	5.42E−04
Human non-carcinogenic toxicity	kg 1,4-DCB	6.31E+ 00	6.31E+ 00	7.57E−01	1.20E+ 01	4.82E+ 00	7.80E+ 00	7.57E−03
Ionizing radiation	kBq Co−60 eq	2.29E−01	2.30E−01	2.20E−01	9.63E+ 01	−2.08E−01	6.58E−01	2.20E−03
Land use	m^2a crop eq	5.20E−02	5.19E−02	1.29E−02	2.48E+ 01	2.67E−02	7.74E−02	1.29E−04
Marine ecotoxicity	kg 1,4-DCB	1.94E+ 00	1.94E+ 00	5.68E−02	2.93E+ 00	1.83E+ 00	2.05E+ 00	5.68E−04
Marine eutrophication	kg N eq	1.11E−04	1.11E−04	3.14E−05	2.84E+ 01	4.85E−05	1.72E−04	3.14E−07
Mineral resource scarcity	kg Cu eq	3.05E−02	3.05E−02	1.96E−03	6.43E+ 00	2.66E−02	3.44E−02	1.96E−05
Ozone formation, Human health	kg NOx eq	3.38E−03	3.38E−03	2.04E−03	6.03E+ 01	−6.17E−04	7.42E−03	2.04E−05
Ozone formation, Terrestrial ecosystems	kg NOx eq	3.50E−03	3.49E−03	2.20E−03	6.30E+ 01	−8.32E−04	7.85E−03	2.20E−05
Stratospheric ozone depletion	kg CFC11 eq	5.14E−07	5.15E−07	2.13E−07	4.13E+ 01	9.35E−08	9.29E−07	2.13E−09
Terrestrial acidification	kg SO_2 eq	4.71E−03	4.70E−03	2.88E−03	6.11E+ 01	−9.42E−04	1.04E−02	2.88E−05
Terrestrial ecotoxicity	kg 1,4-DCB	6.06E+ 00	6.06E+ 00	6.07E−01	1.00E+ 01	4.86E+ 00	7.27E+ 00	6.07E−03
Water consumption	m^3	2.93E−02	2.92E−02	2.45E−02	8.37E+ 01	−1.91E−02	7.74E−02	2.45E−04
Paper industry								
Fine particulate matter formation	kg PM2.5 eq	7.87E−04	7.79E−04	1.07E−03	1.36E+ 02	−1.30E−03	2.89E−03	1.07E−05
Fossil resource scarcity	kg oil eq	1.14E−01	1.11E−01	7.85E−01	6.91E+ 02	−1.44E+ 00	1.64E+ 00	7.85E−03
Freshwater ecotoxicity	kg 1,4-DCB	6.39E−01	6.40E−01	4.47E−02	6.99E+ 00	5.50E−01	7.26E−01	4.47E−04
Freshwater eutrophication	kg P eq	3.82E−04	3.83E−04	4.42E−04	1.16E+ 02	−4.93E−04	1.25E−03	4.42E−06
Global warming	kg CO_2 eq	4.14E−01	4.02E−01	1.20E+ 00	2.91E+ 02	−1.95E+ 00	2.76E+ 00	1.20E−02
Human carcinogenic toxicity	kg 1,4-DCB	2.51E−01	2.51E−01	5.40E−02	2.15E+ 01	1.44E−01	3.57E−01	5.40E−04
Human non-carcinogenic toxicity	kg 1,4-DCB	2.45E+ 00	2.45E+ 00	7.53E−01	3.07E+ 01	9.72E−01	3.93E+ 00	7.53E−03
Ionizing radiation	kBq Co−60 eq	6.25E−02	6.32E−02	2.19E−01	3.50E+ 02	−3.69E−01	4.90E−01	2.19E−03
Land use	m^2a crop eq	1.94E−02	1.94E−02	1.28E−02	6.63E+ 01	−5.80E−03	4.45E−02	1.28E−04
Marine ecotoxicity	kg 1,4-DCB	7.75E−01	7.75E−01	5.65E−02	7.29E+ 00	6.63E−01	8.83E−01	5.65E−04
Marine eutrophication	kg N eq	3.59E−05	3.59E−05	3.12E−05	8.68E+ 01	−2.58E−05	9.71E−05	3.12E−07
Mineral resource scarcity	kg Cu eq	1.21E−02	1.21E−02	1.97E−03	1.62E+ 01	8.24E−03	1.60E−02	1.97E−05
Ozone formation, Human health	kg NOx eq	1.22E−03	1.20E−03	2.04E−03	1.67E+ 02	−2.81E−03	5.22E−03	2.04E−05
Ozone formation, Terrestrial ecosystems	kg NOx eq	1.26E−03	1.24E−03	2.21E−03	1.75E+ 02	−3.10E−03	5.57E−03	2.21E−05
Stratospheric ozone depletion	kg CFC11 eq	1.78E−07	1.78E−07	2.11E−07	1.19E+ 02	−2.39E−07	5.92E−07	2.11E−09
Terrestrial acidification	kg SO_2 eq	1.64E−03	1.62E−03	2.88E−03	1.75E+ 02	−3.92E−03	7.28E−03	2.88E−05
Terrestrial ecotoxicity	kg 1,4-DCB	2.37E+ 00	2.37E+ 00	6.05E−01	2.55E+ 01	1.18E+ 00	3.57E+ 00	6.05E−03
Water consumption	m^3	8.75E−03	8.71E−03	2.43E−02	2.78E+ 02	−3.92E−02	5.66E−02	2.43E−04

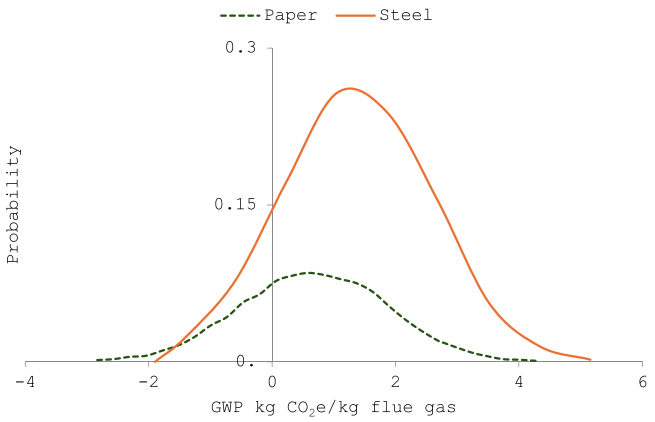

Fig. 11. GWP Monte Carlo simulation results due to variations in the amounts of electricity, ethylene oxide, oxygen and carbon dioxide inputs (with normal distribution with ±10 % standard deviation) for the paper and steel industries' cradle-to-gate flue gas utilization systems.

5.57 and 7.51 kg CO_2e/kg products for the paper and steel industries' flue gas utilization systems. With the economic allocation of the total GWP to AE7, the GWP becomes 11.6 and 16.3 kg CO_2e/kg AE7 for the paper and steel industries' flue gas utilization systems. Thus, the economic allocation results are unfeasible compared to the baseline systems ranging 2.19–3.6 kg CO_2e/kg surfactant (Fig. 3).

As the mass allocation model makes the CO_2 reuse to produce AE7 viable, further mass allocation scenarios are explored per unit carbon utilization (Eq. 3). The total GWP is presented per unit of CO_2 and CO in the flue gas. Then, the carbon utilization factor is incorporated to present GWP per unit of CO_2 and CO utilization.

$$GWP(kgCO_2eper\ kg\ of CO_2and\ CO\ utilisation) = \frac{Total\ GWP\ in\ kgCO_2e}{kg\ flue\ gas} \times \frac{kg\ flue\ gas}{kgCO_2and\ CO\ in\ flue\ gas} \times Carbon\ utilization\ factor \quad (3)$$

The allocations that show lower GWP than the baseline scenarios are highlighted in green. The steel industry's flue gas utilization system has higher environmental impacts due to the higher energy used for heating to make the reactants for AE7 synthesis. As the new systems are integrated into the supply chains, the apparent mass loss, waste, or emission would decrease. Emissions or waste would become feedstock to another industry. The economically allocated LCIA results would then be closer to the mass allocation results, making the system more viable in the future.

A Monte Carlo (MC) simulation with 10,000 runs [75] has been conducted to show their impact on GWP and other impact categories and to what extent these impacts can be lowered. The multi-variate uncertainty analysis is conducted on the most significant flows or hotspots because of their greater influences on the life cycle impacts. The amounts of oxygen, ethylene oxide, carbon dioxide and electricity inputs were varied according to the normal distribution with a ±10 % standard deviation. Table 7 shows the full MC simulation results in terms of standard deviation (SD), coefficient of variance (CV) and standard error mean (SEM) of ReCiPe (M) (H) profiles of the steel and paper industry. SD is a measure of how spread out the numbers in a set are. It shows how much the values differ from the average (mean) value. A low standard deviation means the numbers are close to the average, while a high standard deviation means they are spread out over a wider range. CV measures how much variation or spread there is in a set of data, relative to the average (mean). It's calculated by dividing the SD by the mean and multiplying by 100 to get a percentage. In simple terms, the CV helps compare the variability between different sets of data, even if they have different units or scales. A lower CV means less variability, while a higher CV means more variability relative to the average. SEM is a measure of how much the average (mean) of a sample is likely to differ from the true average of the entire population. It shows the accuracy of the sample mean in estimating the population mean. In simple terms, SEM tells how reliable the sample mean is. A smaller SEM means the sample mean is closer to the true population mean, while a larger SEM suggests more variation or less reliability in the estimate. It's calculated by dividing the standard deviation of the sample by the square root of the sample size.

It can be seen from Table 7 that apart from GWP, the other ReCiPe (M) (H) LCIA values are robust or certain. Thus, the GWP distributions are further examined. The amounts of electricity, ethylene oxide, oxygen and carbon dioxide inputs were varied simultaneously according to the normal distribution with a ±10 % standard deviation to generate the GWP distribution profile in Fig. 11. As a consequence, GWP (kg CO_2e/kg flue gas) would vary significantly between −1.05 and 3.73 (at ±97.5 % SD) for the steel industry and −1.95 and 2.76 (at ±97.5 % SD) for the paper industry. The results give the confidence that the GWP reduction can fall within the baseline systems' range (<3.6 kg CO_2e/kg surfactant).

The paper industries' flue gas utilization system has a higher spread or greater uncertainty than the steel industries' flue gas utilization system. Thus, the CV is greater in the former than in the latter. There is a 90 % probability of steel industries' cradle-to-gate flue gas utilization system's GWP falling below 2.1 kg CO_2e/kg flue gas. There is an 85 % probability of paper industries' cradle-to-gate flue gas utilization system's GWP falling below −0.6 kg CO_2e/kg flue gas. The probability of having a negative GWP is lower than the probability of having a positive GWP for both the cradle-to-gate systems.

Gate-to-grave GWP: Surfactants are designed to biodegrade after use completely, according to regulations. The AE7 product contains biodegradable molecules. Thus, when commercialized, the process would lead to marketable biodegradable surfactants. For such products, product

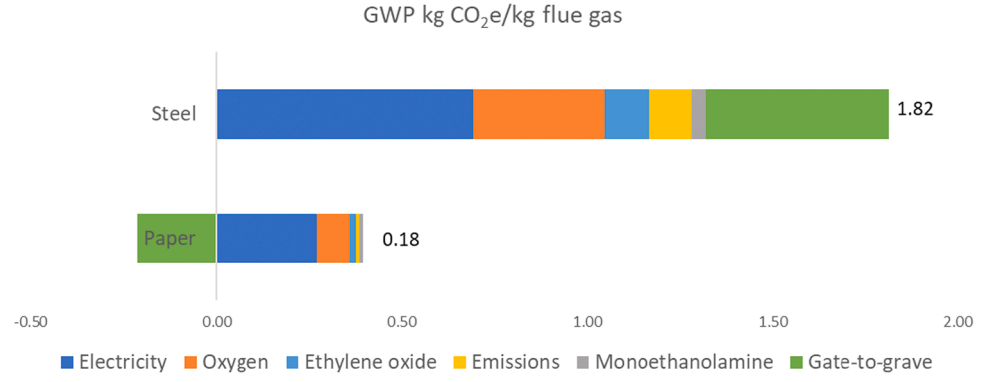

Fig. 12. Cradle-to-grave GWP per unit flue gas of paper and steel industries' flue gas utilization systems.

Table 8
Cradle-to-grave GWP of paper and steel industries' flue gas utilization system. The feasible GWP bases compared to the baseline systems are highlighted.

GWP kg CO_2e	Basis	Paper	Steel
Mass allocation	per kg flue gas	0.18	1.82
Economic allocation to product	per kg product	2.56	10.33
Economic allocation to AE7	per kg AE7	5.34	22.46

environmental footprint requires cradle-to-grave GWP as per the regulations. Thus, the gate-to-grave GWP is calculated and added to the cradle-to-gate GWP (Fig. 10 and Table 6) to obtain the cradle-to-grave GWP. The calculation of the gate-to-grave GWP is as follows. Fig. 8 shows 60 kg and 180 kg of carbon present in the paper and steel industries' flue gases, respectively. Their total carbon utilization is 0.97 and 0.75 (Fig. 8), thus, leading to (60 times 0.97 or) 58.2 kg and (180 times 0.75 or) 135 kg carbon in the useful products (surfactant and fuel), respectively. These amounts correspond to 213.4 and 495 kg CO_2e per tonne flue gas GWP, from their gate-to-grave systems, respectively. The former system's embedded carbon (paper industries' flue gas) is biogenic, while the latter system (steel industries' flue gas) is fossil-based. The biogenic carbon cycle is faster than the fossil-based carbon cycle, as carbon dioxide released into the atmosphere is sequestered during biomass growth closing the biogenic carbon dioxide cycle. The cradle-to-grave GWP of the flue gas system is thus (0.4 (from Fig. 10 and Table 6) subtracted by 0.2134 or) 0.18 and (1.32 (from Fig. 10 and Table 6) added to 0.495 or) 1.82 kg CO_2e GWP per kg flue gas, respectively. Fig. 12 illustrates the negative biogenic carbon dioxide impact resulting in an overall reduced GWP for the cradle-to-grave paper industry's flue gas utilization system (0.18 kg CO_2e GWP per kg flue gas) and the fossil-based carbon dioxide impact resulting in an overall increased GWP for the cradle-to-grave steel industry's flue gas utilization system (1.82 kg CO_2e GWP per kg flue gas). Fig. 12 additionally lays the gate-to-grave GWP on the top of cradle-to-gate GWP in Fig. 10.

Allocating the GWP to the marketable products (surfactant + fuel) makes the paper industries' flue gas utilization via this route still viable, with 2.56 kg CO_2e GWP per kg product because of the biogenic carbon in the product. The steel industries' flue gas utilization via this route becomes infeasible, with 10.33 kg CO_2e GWP per kg product. Table 8 highlights the feasible GWP of the steel and paper industries' flue gas utilization systems.

Thus, both paper and steel CCU/CDU systems are environmentally viable from a flue gas utilisation perspective. From the products' perspective, the paper industry's utilization system is environmentally feasible compared to the baseline systems due to the presence of biogenic carbon dioxide in the feedstock. The comprehensive LCA shows the criticality of biogenic carbon in the product (Table 8) and carbon utilization in the products (Table 6). Biogenic carbon and greater carbon utilization make the paper industries' flue gas system feasible and competitive against baseline existing surfactant production systems.

4. Conclusions

This study presents a novel LCA of alcohol ethoxylate (AE7) production from industrial flue gas. The sustainable process consists of Fischer-Tropsch (FT) technology from our previous work exploiting the Anderson-Schulz-Flory (ASF) distribution model. Flue gas containing carbon dioxide (and carbon monoxide) is converted into produce syngas, which is fed to FT synthesis and hydroprocessing primarily producing C11-C13 alkanes. Alkanes are converted into C12-C14 fatty alcohols via dehydrogenation into olefins, hydroformylation into aldehydes and hydrogenation. A part of the syngas is also converted into ethylene oxide by thermocatalytic conversion via ethanol. Ethylene oxide and C12-C14 fatty alcohols react to make AE7. A middle distillate range gasoline-to-diesel fraction is also extracted from FT. Detailed and comprehensive LCA analyses of baseline cases are shown to note their cradle-to-gate GWP range, 2.19–3.6 kg CO_2e/kg surfactant. They capture all plausible baseline systems creating a range of impacts to benchmark against. For the new AE7 production system, the LCIA has been reported from CO_2 reuse and AE7 and AE7 plus fuel production perspectives, using mass and economic allocations. Mass-allocated LCIA justifies CO_2 reuse for AE7 synthesis, i.e., the cradle-to-gate for the paper and steel industries' utilization systems (0.4 and 1.32 kg CO_2e/kg flue gas). They are also viable based on plausible mass allocation, i.e., per kg CO_2 and CO in flue gas or utilization. Economically, LCIA allocated to the product (AE7 plus fuel) shows feasibility for paper industry CO_2 utilization within baseline scenarios. Given the added-value AE7 surfactant product's yield is very low, co-product recovery is key for the system's environmental feasibility. The hotspots in the new AE7 production system are electricity use for heat and reactant hydrogen supplies required to produce the C12-C14 fatty alcohol and ethylene oxide for AE7 synthesis. Biogenic CO_2 present in the industrial flue gas makes AE7 production more environmentally benign. The paper industry's flue gas system is biogenic, while the steel industry's is fossil-based, resulting in 2.56 kg CO_2e and 10.33 kg CO_2e GWP per kg product (AE7 +Fuel), respectively, for the cradle-to-grave systems. Thus, biogenic CDU/CCU is a climate-efficient way to displace fossil-based commodities.

CRediT authorship contribution statement

Jhuma Sadhukhan: Writing – original draft, Visualization, Validation, Software, Methodology, Investigation, Data curation, Conceptualization. **Benjamin Cummings:** Writing – original draft, Visualization. **Oliver Fisher:** Writing – original draft, Visualization, Software, Methodology, Formal analysis, Data curation. **Jin Xuan:** Writing – review & editing, Supervision, Resources, Project administration, Methodology, Investigation, Funding acquisition.

Declaration of Competing Interest

The authors declare that they have no known competing financial interests or personal relationships that could have appeared to influence the work reported in this paper.

Acknowledgements

The authors gratefully acknowledge the funding support of Innovate UK under grant number TS/X017648/1 https://www.soci.org/news/2023/1/flue2chem-sci-unilever-and-13-partners-launch-net-zero-collaboration-project to support this work.

Appendix A. Supporting information

Supplementary data associated with this article can be found in the online version at doi:10.1016/j.jcou.2024.103013.

Data availability

All data assumptions are included

References

[1] Allied Market Research. ⟨https://www.alliedmarketresearch.com/surfactant-market⟩ (2023).
[2] G.O. Reznik, P. Vishwanath, M.A. Pynn, J.M. Sitnik, J.J. Todd, J. Wu, Y. Jiang, B. G. Keenan, A.B. Castle, R.F. Haskell, T.F. Smith, Appl. Microbiol. Biotechnol. 86 (2010) 1387–1397.
[3] A.J.K. Newman, G.R.M. Dowson, E.G. Platt, H.J. Handford-Styring, P. Styring, Front Energy Res 11 (2023).
[4] Y.A. Alassmy, K.O. Sebakhy, F. Picchioni, P.P. Pescarmona, J. CO2 Util. 50 (2021) 101577.
[5] J. Young, N. McQueen, C. Charalambous, S. Foteinis, O. Hawrot, M. Ojeda, H. Pilorgé, J. Andresen, P. Psarras, P. Renforth, S. Garcia, One Earth 6 (7) (2023) 899–917.
[6] Ursula Balderson, Vera Trappmann & Jo Cutter. Decarbonising the Foundation Industries and the Implications for Workers and Skills in the UK. (2022).
[7] A. Saravanan, D.V.N. Vo, S. Jeevanantham, V. Bhuvaneswari, V.A. Narayanan, P. R. Yaashikaa, S. Swetha, B. Reshma, Chem. Eng. Sci. 236 (2021) 116515.
[8] A. Nisar, S. Khan, M. Hameed, A. Nisar, H. Ahmad, S.A. Mehmood, Microbiol. Res. 251 (2021) 126813.
[9] K. Markandan, R. Sankaran, Y.Wei Tiong, H. Siddiqui, M. Khalid, S. Malik, S. Rustagi, Catalysts 13 (2023) 611.
[10] R.J. Detz, C.J. Ferchaud, A.J. Kalkman, J. Kemper, C. Sánchez-Martínez, M. Saric, M.V. Shinde, Sustain Energy Fuels 7 (23) (2023) 5445–5472.
[11] K.S. Ng, N. Zhang, J. Sadhukhan, Chem. Eng. J. 219 (2013) 96–108.
[12] Q. Zhang, M. Bown, L. Pastor-Pérez, M.S. Duyar, T.R. Reina, Ind. Eng. Chem. Res 61 (2022) 12857–12865.
[13] A.D.N. Kamkeng, M. Wang, J. Hu, W. Du, F. Qian, Chem. Eng. J. 409 (2021) 128138.
[14] G. Zang, P. Sun, A.A. Elgowainy, A. Bafana, M.J. Wang, CO2 Util. 46 (2021) 101459.
[15] A. Galadima, O. Muraza, Ren. Sustain. Energy Rev. 115 (2019) 109333.
[16] Z. Navas-Anguita, P.L. Cruz, M. Martín-Gamboa, D. Iribarren, J. Dufour, Fuel 235 (2019) 1492–1500.
[17] G. Zang, P. Sun, A. Elgowainy, A. Bafana, M. Wang, Environ. Sci. Technol. 55 (2021) 3888–3897.
[18] Y. He, L. Zhu, J. Fan, L. Li, G. Liu, Fuel Process. Technol. 221 (2021) 106924.
[19] G. Zang, P. Sun, A.A. Elgowainy, A. Bafana, M. Wang, J. CO2 Util. 46 (2021) 101459.
[20] C.M. Liu, N.K. Sandhu, S.T. McCoy, J.A. Bergerson, Sustain. Energy Fuels 4 (2020) 3129–3142.
[21] J. Artz, T.E. Müller, K. Thenert, J. Kleinekorte, R. Meys, A. Sternberg, A. Bardow, W. Leitner, Chem. Rev. 118 (2) (2018) 434–504.
[22] A. Sternberg, C.M. Jens, A. Bardow, Green. Chem. 19 (9) (2017) 2244–2259.
[23] M. Shemfe, S. Gadkari, E. Yu, S. Rasul, K. Scott, I.M. Head, S. Gu, J. Sadhukhan, Bioresour. Technol. 255 (2018) 39–49.
[24] S. Gadkari, B.H.M. Beigi, N. Aryal, J. Sadhukhan, RSC Adv. 11 (17) (2021) 9921–9932.
[25] S.K. Nabil, S. McCoy, M.G. Kibria, Green. Chem. 23 (2) (2021) 867–880.
[26] N. Meunier, R. Chauvy, S. Mouhoubi, D. Thomas, G. De Weireld, Renew. Energy 146 (2020) 1192–1203.
[27] R. Chauvy, R. Lepore, P. Fortemps, G. De Weireld, Sustain. Prod. Consum. 24 (2020) 194–210.
[28] S. Perdan, C.R. Jones, A. Azapagic, Public awareness and acceptance of carbon capture and utilisation in the UK, Sustain. Prod. Consum. 10 (2017) 74–84.
[29] H. Liu, Y. Tang, X. Ma, J. Tang, W. Yue, Biomass gasification based on sorption-enhanced hydrogen production coupled with carbon utilization to produce tunable syngas for methanol synthesis, Energy Convers. Manag. 309 (2024) 118428.
[30] N. Wubulikasimu, R. Shen, L. Hao, H. He, K. Li, X. Li, J. Xie, Selective CO2 hydrogenation to methanol over a novel ternary In-Co-Zr catalyst, Chem. Eng. J. 501 (2024) 157397.
[31] J. Palomo, M.Á. Rodríguez-Cano, J. Rodríguez-Mirasol, T. Cordero, Biomass-derived activated carbon catalysts for the direct dimethyl ether synthesis from syngas, Fuel 365 (2024) 131264.
[32] L. Vaquerizo, A.A. Kiss, Thermally self-sufficient process for single-step coproduction of methanol and dimethyl ether by CO2 hydrogenation, J. Clean. Prod. 441 (2024) 140949.
[33] O.J. Fisher, J. Sadhukhan, T. Daniel, J. Xuan, Techno-economic analysis and process simulation of alkoxylated surfactant production in a circular carbon economy framework, Digit. Chem. Eng. (2024) 100199, https://doi.org/10.1016/j.dche.2024.100199.
[34] K. Onarheim, S. Santos, P. Kangas, V. Hankalin, Int. J. Greenh. Gas. Control 59 (2017) 58–73.
[35] J. Collis, T. Strunge, B. Steubing, A. Zimmermann, R. Schomäcker, Front Energy Res 9 (2021).
[36] B. Aghel, S. Janati, S. Wongwises, M.S. Shadloo, Int. J. Greenh. Gas. Control 119 (2022) 103715.
[37] S. Akhbarifar, M. Shirvani, Chem. Eng. Res. Des. 147 (2019) 483–492.
[38] J. Sadhukhan, K.S. Ng, E. Martinez-Hernandez, Biorefineries & Chemical Processes: Design, Integration and Sustainability Analysis, Wiley UK, 2014 doi:10.1002/9781118698129.
[39] G. Zang, S. Tejasvi, A. Ratner, E.S. Lora, Bioresour. Technol. 255 (2018) 246–256.
[40] P. Spath, A. Aden, T. Eggeman, M. Ringer, B. Wallace, J. Jechura, Biomass to hydrogen production detailed design and economics utilizing the Battelle Columbus Laboratory indirectly-heated gasifier (No. NREL/TP-510-37408). National Renewable Energy Lab. (NREL) Golden CO (United States) (2005). doi: 10.2172/15016221.
[41] X. Su, X. Yang, B. Zhao, Y. Huang, J. Energy Chem. 26 (2017) 854–867.
[42] D.H. Kim, J.L. Park, E.J. Park, Y.D. Kim, S. Uhm, ACS Catal. 4 (2014) (2014) 3117–3122.
[43] N.R. Sukor, A.H. Shamsuddin, T.M.I. Mahlia, M.F.Mat Isa, Processes 8 (2020) 350.
[44] K.S. Ng, J. Sadhukhan, Biomass-.-. Bioenergy 35 (2011) 3218–3234.
[45] R. Peters, N. Wegener, R.C. Samsun, F. Schorn, J. Riese, M. Grünewald, D. Stolten, Processes 10 (4) (2022) 699.
[46] C. Bouchy, G. Hastoy, E. Guillon, J.A. Martens, Fischer-Tropsch Waxes Upgrading Hydrocracking and Selective Hydroisomerization, Oil Gas. Sci. Technol. - Rev. De. l'IFP 64 (2009) 91–112.
[47] J. Sadhukhan, S. Sen, Chem. Eng. Res. Des. 175 (2021) 358–379.
[48] J. Sadhukhan, K.S. Ng, Ind. Eng. Chem. Res. 50 (11) (2011) 6794–6808.
[49] M. Findlater, J. Choi, A.S. Goldman, M. Brookhart, Alkane Dehydrogenation, in: P. Pérez (Ed.), Alkane C-H Activation by Single-Site Metal Catalysis. Catalysis by Metal Complexes, 38, Springer, Dordrecht, 2012 https://doi.org/10.1007/978-90-481-3698-8_4.
[50] R. Franke, D. Selent, A. Börner, Chem. Rev. 112 (11) (2012) 5675–5732.
[51] T.L. Zebert, D. Lokhat, S. Kurella, B.C.S. Meikap, Afr. J. Chem. Eng. 43 (2023) 204–214.
[52] M.H. Barecka, M. Skiborowski, A. Górak, Chem. Eng. Res. Des. 123 (2017) 295–316.
[53] C.B. Mukta, N.R. Rayaprolu, S. Cremaschi, M.R. Eden, B.J. Tatarchuk, Techno-Econ. Study Intensified Ethyl. Oxide Prod. Using High. Therm. Conduct. Micro Entrapped Catal. (2022) 697–702, https://doi.org/10.1016/B978-0-323-85159-6.50116-0.
[54] R. Tesser, V. Russo, E. Santacesaria, W. Hreczuch, M. Di Serio, Front. Chem. Eng. 2 (2020).
[55] K.G. McDaniel, High. Product. alkoxylation Process. (2007).
[56] Y.M. Lim, V. Swamy, N. Ramakrishnan, E.S. Chan, H.P. Kesuma, Microchem. J. 195 (2023) 109537.
[57] N.A. Rahman, C. Jose Jol, A.A. Linus, D.S. Rozellia Kamel Sharif, V. Ismail, Case Stud. Chem. Environ. Eng. 3 (2021) 100106.
[58] E. Martinez-Hernandez, J. Martinez-Herrera, G.M. Campbell, J. Sadhukhan, Biomass-.-. Conv. Biorefinery 4 (2014), 105-100124.
[59] J. Sadhukhan, S. Sen, S. Gadkari, J. Clean. Prod. (2021) 127457.
[60] J. Sadhukhan, Renew. Energy 184 (2022) 960–974.
[61] R.I. Muazu, J. Sadhukhan, S.V. Mohan, S. Gadkari, Environ. Sci: Water Res. Technol. 9 (10) (2023) 2487–2500.
[62] M. Courtat, P.J. Joyce, S. Sim, J. Sadhukhan, R. Murphy, J. Environ. Manag. 336 (2023) 117684.
[63] J. Sadhukhan, Energies 15 (15) (2022) 5522.
[64] S. Wang, F. Li, J. Sadhukhan, J. Xuan, X. Mao, L. Xing, X. Zhao, X. Wang, J. Clean. Prod. 434 (2024) 139846.
[65] R.H. Hafyan, J. Mohanarajan, M. Uppal, V. Kumar, V. Narisetty, S.K. Maity, J. Sadhukhan, S. Gadkari, Energy Conv. Manag. 301 (2024) 118033.
[66] ⟨https://ecoinvent.org/ecoinvent-v3-10/⟩.
[67] ⟨https://www.erasm.org/wp-content/uploads/2022/07/9-ERASM-Environmental-Fact-Sheet-C12-14-AE3.pdf⟩.
[68] J. Sadhukhan, S. Sen, T.M.S. Randriamahefasoa, S. Gadkari, Digit. Chem. Eng. 3 (2022) 100026.
[69] J. Sadhukhan, M. Christensen, Energies 14 (17) (2021) 5555.
[70] J. Sadhukhan, B.G. Pollet, M. Seaman, Energies 15 (15) (2022) 5486.
[71] J. Sadhukhan, J.R. Lloyd, K. Scott, G.C. Premier, H.Y. Eileen, T. Curtis, I.M. Head, Ren. Sustain. Energy Rev. 56 (2016) 116–132.
[72] E. Martinez-Hernandez, J. Sadhukhan, J. Aburto, M.A. Amezcua-Allieri, S. Morse, S.R. Murphy, Clean. Technol. Environ. Policy (2022) 1–17.
[73] Y.K. Wan, J. Sadhukhan, K.S. Ng, D.K. Ng, Chem. Eng. Res. Des. 107 (2016) 263–279.
[74] P. Thanahiranya, J. Sadhukhan, P. Charoensuppanimit, A. Soottitantawat, A. Arpornwichanop, N. Thongchul, S. Assabumrungrat, ACS Sustain. Chem. Eng. 11 (49) (2023) 17425–17439.
[75] J. Sadhukhan, Appl. Energy 122 (2014) 196–206.